

In Vivo Multiphoton Microscopy for Investigating Biomechanical Properties of Human Skin

XING LIANG,¹ BENEDIKT W. GRAF,¹ and STEPHEN A. BOPPART²

¹Department of Electrical and Computer Engineering, Biophotonics Imaging Laboratory, Beckman Institute for Advanced Science and Technology, University of Illinois at Urbana-Champaign, 405 North Mathews Avenue, Urbana, IL 61801, USA; and ²Departments of Electrical and Computer Engineering, Bioengineering, and Medicine, Biophotonics Imaging Laboratory, Beckman Institute for Advanced Science and Technology, University of Illinois at Urbana-Champaign, 405 North Mathews Avenue, Urbana, IL 61801, USA

(Received 28 May 2010; accepted 30 October 2010)

Associate Editor Yingxiao Wang Peter J. Butler oversaw the review of this article.

Abstract—The biomechanical properties of living cells depend on their molecular building blocks, and are important for maintaining structure and function in cells, the extracellular matrix, and tissues. These biomechanical properties and forces also shape and modify the cellular and extracellular structures under stress. While many studies have investigated the biomechanics of single cells or small populations of cells in culture, or the properties of organs and tissues, few studies have investigated the biomechanics of complex cell populations *in vivo*. With the use of advanced multiphoton microscopy to visualize *in vivo* cell populations in human skin, the biomechanical properties are investigated in a depth-dependent manner in the stratum corneum and epidermis using quasi-static mechanical deformations. A 2D elastic registration algorithm was used to analyze the images before and after deformation to determine displacements in different skin layers. In this feasibility study, the images and results from one human subject demonstrate the potential of the technique for revealing differences in elastic properties between the stratum corneum and the rest of the epidermis. This interrogational imaging methodology has the potential to enable a wide range of investigations for understanding how the biomechanical properties of *in vivo* cell populations influence function in health and disease.

Keywords—Multiphoton microscopy, Imaging, Cell and tissue biomechanics, Human skin, *In vivo*.

INTRODUCTION

Cellular biomechanics has been an active area of research for the past several decades, led by the

development of new investigational tools and techniques. At the cellular level, mechanical forces play a significant role in guiding cell functions as they are actively sensed by living cells. Cell and tissue responses to mechanical stimuli frequently result in adaptive changes that modulate form and function. When such mechanical forces and cues are absent or erroneous, structural and functional derangements may occur, such as inducing cells into an abnormal state.² For example, the biomechanical properties of tumor cells change during the development and metastasis of cancer.

Researchers have conducted studies measuring the biomechanical properties of single cells and *in vitro* cell populations. For instance, single cell biomechanical properties were estimated using mechanical excitations. Atomic force microscopy (AFM) and magnetic twisting cytometry (MTC) have been used as methods in which a portion of the cell is deformed.^{4,23} Micropipette aspiration has been used to deform a cell by applying suction on the cell membrane, and optical tweezers have been used to apply forces on adherent beads to deform a cell.^{10,29} In addition to measurements of specific mechanical properties, mechanical models have been developed to study the mechanical properties of single cells, including tensegrity models and cellular solids models.^{3,5,27}

Recent efforts are interested in understanding more complex cell dynamics in cell populations, and micro-fabricated systems have been used to record traction forces generated by a cell population.^{20,21} Studies have also revealed that the extracellular matrix has a significant role and effect on cell populations.¹² However, most experimental studies have focused on cellular biomechanics *in vitro*, which are most likely to be very different from the cellular biomechanics in living tissues.

Address correspondence to Stephen A. Boppart, Departments of Electrical and Computer Engineering, Bioengineering, and Medicine, Biophotonics Imaging Laboratory, Beckman Institute for Advanced Science and Technology, University of Illinois at Urbana-Champaign, 405 North Mathews Avenue, Urbana, IL 61801, USA. Electronic mail: boppart@illinois.edu

In vivo biomechanics at the level of organs and tissues have been investigated using modern technologies, especially on human skin for morphological, medical, and cosmetic purposes. For example, digital image correlation has been used for human skin displacement detection²² and improvements in basal cell carcinoma detection have been made based on variations in the biomechanical properties of skin.¹⁶ A study investigating age-related skin changes in mechanical properties has also been performed based on speckle correlation.²⁸ However, most of these techniques concentrate on imaging the skin surface, neglect depth-dependent information, and lack the ability to resolve cellular features and the dynamics of cell populations. Skin mechanics depend significantly on the dynamic cellular morphology and microenvironment of deeper skin layers, as well as the outer-most stratum corneum, which is mainly composed of dead cells, but provides a protective barrier function. Cross-sectional imaging technologies such as ultrasound and optical coherence tomography have been utilized to study depth-dependent skin biomechanical properties,^{8,18} but resolution and contrast limitations have restricted these imaging modalities to extracting more tissue-level biomechanics from skin. The use of reflectance confocal microscopy has been successfully demonstrated for imaging cellular features in *in vivo* human skin,^{6,25} however, few studies have integrated mechanical excitations with confocal microscopy to investigate the biomechanical properties of cell populations in living skin.

Multiphoton microscopy (MPM) is a high-resolution imaging technique that relies on the non-linear excitation of endogenous or exogenous fluorescent molecules, and has been widely applied to investigate human skin *in vivo* including skin cancer diagnosis,⁷ skin aging,¹³ and drug monitoring,¹⁴ among many other applications. In this technical feasibility study, we present a method to study the biomechanical properties of human skin on the cellular level using MPM. Images and data were collected from one human subject, and the biomechanical properties were estimated for the different skin layers applying quasi-static external mechanical perturbations. To the best of our knowledge, this is the first experimental demonstration of depth-dependent cell population biomechanics in *in vivo* human skin.

MATERIALS AND METHODS

Multiphoton Microscopy System

For this study, a custom built integrated microscope system was used, which had been introduced in a

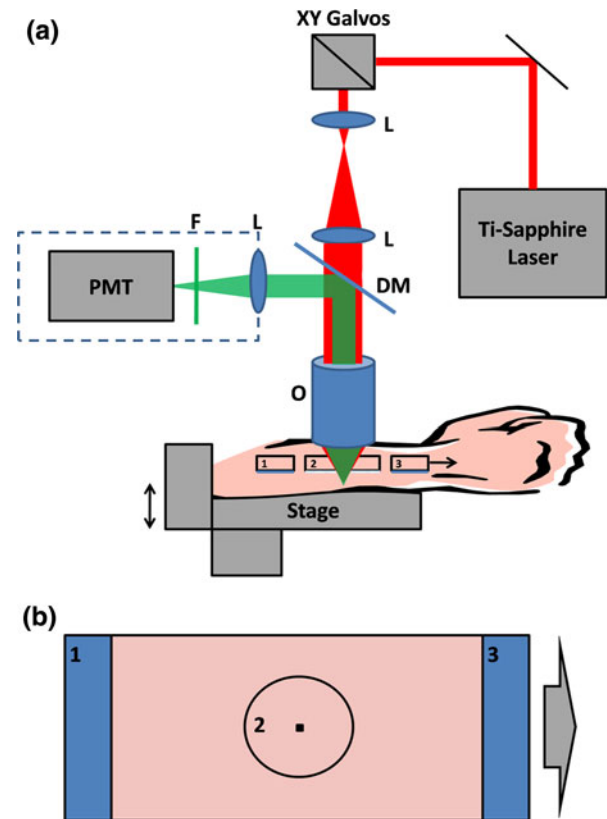


FIGURE 1. Schematic of the multiphoton microscope used to image *in vivo* human skin. (a) The forearm was mounted on a motorized vertical stage, and the skin region to be imaged was fixed to coverslip 1 and 3 using double-sided tape. MPM images were acquired through the imaging window 2. A thin film of glycerin applied to the skin served as a lubricant between the skin surface and this window. (b) For biomechanical property measurements, a quasi-static lateral deformation was applied to coverslip 3 and the adherent skin. The surface area of skin that was deformed was $40\text{ mm} \times 20\text{ mm}$, and the image FOV (small black square) under the imaging window 2 was at most $600\text{ }\mu\text{m} \times 600\text{ }\mu\text{m}$ for the MPM mosaics. DM, dichroic mirror; F, filter; L, lens; O, objective; PMT, photomultiplier tube.

previous study.¹¹ This multi-channel microscope enables structural cell and tissue imaging utilizing optical coherence microscopy and functional imaging utilizing MPM.^{19,31} Real-time A-scans from optical coherence microscopy images were used to locate the skin surface, and MPM microscopy was used for skin imaging. The schematic of the MPM system is shown in Fig. 1. The MPM system is based on a tunable Ti-Sapphire laser (Mai Tai, Spectra Physics), which has a center wavelength of 770 nm, bandwidth of 12 nm, a pulse width of 150 fs, and a repetition rate of 80 MHz. The beam passes through a pair of scanning galvanometers and is expanded by a telescope to fill the back aperture of a $20\times$, 0.95NA water immersion objective (Olympus) with a working distance of $\sim 1.5\text{ mm}$. The focused light, with a mean excitation

power of ~ 20 mW, generates a two-photon fluorescence signal from the sample, which is collected by the objective and directed to the detector using a dichroic mirror (Cold Mirror, CVI laser). The system parameters are comparable to those for a class I M device according to the European laser safety regulations.¹⁵ The detector consists of a photomultiplier tube (PMT) and filter to block the pump light. *En face* images are formed by detecting the raster scanned beam while focus depth is changed by the motorized stage on which the skin site is positioned. Acquisition time is ~ 4 s for one *en face* image with a field of view (FOV) of $260 \mu\text{m} \times 260 \mu\text{m}$, and ~ 10 min for one 3D image stack.

Human Subject Measurement

All *in vivo* MPM imaging experiments were performed on the left inner forearm skin of a healthy male volunteer under room temperature and humidity. This study was conducted using procedures and protocols that were reviewed and approved by the Institutional Review Board at the University of Illinois at Urbana-Champaign. Informed consent was obtained from the subject prior to imaging. The experiments consisted of measurements under two different states, namely under normal and hydrated skin conditions, to demonstrate the feasibility of this method for detecting changes in the biomechanical properties of *in vivo* tissue. The hydrated state was produced by immersing the skin in a water bath for 20 min, followed by a topical application of glycerin (G33-500, Fisher Scientific).

Experimental Procedure

MPM was first used to detect cellular features and cell populations in *in vivo* human skin. An image mosaic $600 \mu\text{m} \times 600 \mu\text{m}$ in size was acquired by combining 16 MPM images of $160 \mu\text{m} \times 160 \mu\text{m}$ FOV at each imaging depth. Once cellular features were identified, MPM was then used to assess the biomechanical properties of the skin. At each skin region of interest, 3D stacks of MPM images with a FOV of $260 \mu\text{m} \times 260 \mu\text{m}$ were taken before and after a uniaxial deformation was applied. As shown in Fig. 1, the left arm of the volunteer was positioned on the stage and against the imaging window. During the experiments, the skin was held fixed at one end by double-sided tape to coverslip 1, and was stretched at the other end, which was fixed to coverslip 3 by double-sided tape. Images were taken through coverslip 2 and a layer of glycerin applied to the surface of the skin, which also acted as a lubricant between the imaging window and the skin. The three coverslips were fixed to the stage separately, and were adjusted at the same

height against the skin surface. Over the region of interest on the skin (40 mm long and 20 mm wide), coverslip 2 was positioned in the center as the imaging window. The lateral translation of coverslip 3 (delivered by a translational stage) provided a strain of 2.5% (1 mm displacement). After the deformation of the skin was performed, real-time A-scan optical coherence microscopy data was collected and used to locate the skin surface, so that the 3D MPM image stacks before and after deformation were co-registered and contained the same depth-dependent cell population layers within the region of interest.

Image Processing

At each depth within the acquired 3D MPM image stacks, the response of the skin was determined by elastic deformation to the uniaxial stretch. To assess the deformation between images at one depth, an image registration algorithm (bUnwarpJ plug-in, ImageJ) was used. The details of this algorithm are introduced elsewhere.²⁶ Briefly, the skin images before deformation were considered as target images, while the images after deformation were considered as source images. The deformation field was modeled as a B-spline function, determined by minimizing a pixel-wise mean-square distance measure between the target and the source images, and constrained by a vector-spline regularization. Once the deformation field was determined, it was then decomposed to yield average displacements along and across the deformation direction at one depth. The average displacements over depth were used as quantitative results of skin responses and were used to analyze the skin biomechanical properties. The MPM image stacks before and after deformation were also reconstructed to demonstrate volumetric features of *in vivo* human skin using Amira[®] software (Visage Imaging, Inc., San Diego, CA).

RESULTS AND DISCUSSION

Cellular Features From Multiphoton Microscopy of In Vivo Human Skin

Mosaics of MPM images with larger field of view ($600 \mu\text{m} \times 600 \mu\text{m}$) from *in vivo* human skin were first acquired from different depths to select regions of interest, and are shown in Fig. 2. The skin morphology of normal skin agrees well with MPM images of human skin obtained in other studies.^{9,13} In Fig. 2a, an MPM image at a superficial depth of $3 \mu\text{m}$ is demonstrated. The contrast in this image is primarily due to autofluorescent signals from corneocytes, which have

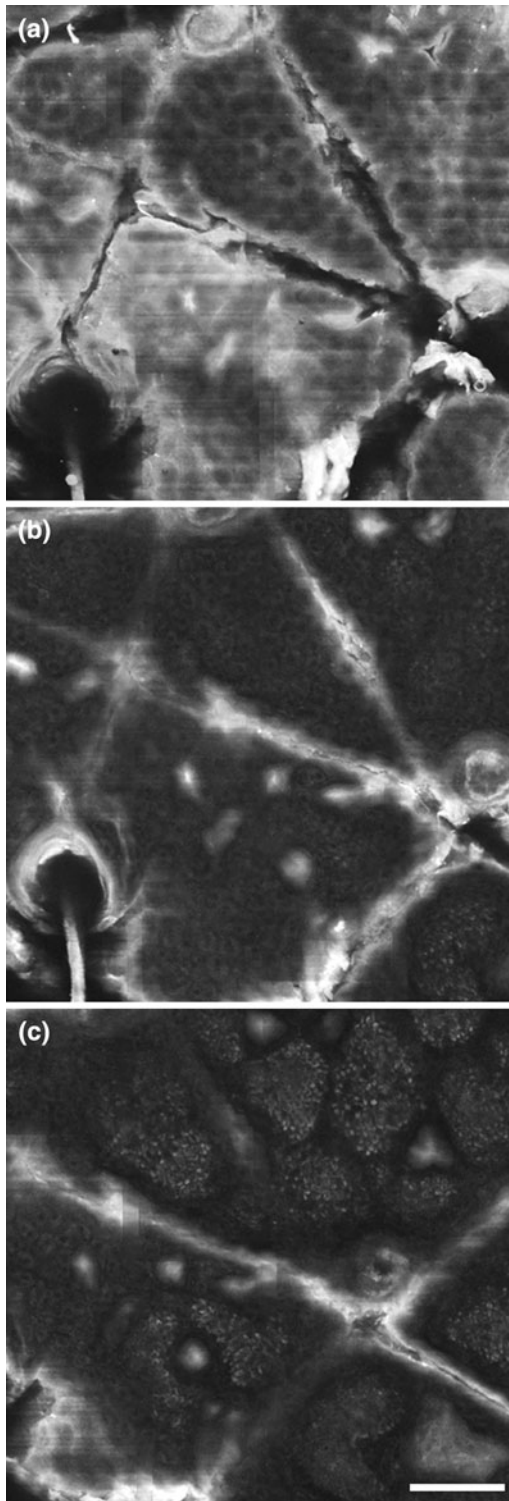


FIGURE 2. Multiphoton microscopy image mosaics of *in vivo* human skin for detecting cellular features at different layers. Mosaics comprised a $600\ \mu\text{m} \times 600\ \mu\text{m}$ area of skin. Imaging depth are (a) $3\ \mu\text{m}$, (b) $13\ \mu\text{m}$, and (c) $23\ \mu\text{m}$. Different cell types and populations are observed at different depths, and a single hair shaft is observed in the lower left corner of the images. Scale bar denotes $100\ \mu\text{m}$ and applies to all images.

the main fluorophore keratin in the stratum corneum layer.²⁴ Microscopic skin furrows and a hair shaft are also discernable in this image. Figure 2b is the MPM mosaic from a depth of $13\ \mu\text{m}$, showing cellular features of the stratum granulosum layer. Cellular features in this layer are characterized by an autofluorescent cytoplasm and nonfluorescent round nuclei,⁹ and the morphological features of the skin furrows and hair shaft are still evident. Figure 2c is the MPM mosaic acquired at a depth of $23\ \mu\text{m}$. In this image, cells in the stratum spinosum layer can be clearly differentiated. Image contrast between the cellular features in this layer is largely due to autofluorescence from NADH.¹³ While these major features dominate each skin layer as illustrated in Fig. 2, there are many other morphological features present within each MPM image from other skin layers, because of the non-planar geometry of the skin layers. Hair shafts were intentionally avoided in the following experiments because the large autofluorescent signal from hair frequently saturated the detector and electronics, making image registration problematic.

Skin Biomechanical Property Analysis

Three-dimensional MPM image stacks of *in vivo* human skin were acquired, and *en face* MPM images at each depth were processed before and after deformation (uniaxial stretch) to yield deformation fields. This process is demonstrated in Fig. 3. Six representative target MPM images acquired before deformation are shown in the left figure column, for imaging depths ranging from 3 to $37\ \mu\text{m}$. Their corresponding source images after the lateral deformation are shown in the right figure column. The elastic image registration algorithm as described above was applied to the image pairs at different depths to yield the deformation fields. Displacement vectors from the deformation fields are overlaid with the target images, as shown in the middle figure column.

The displacement vectors are primarily oriented parallel to the deformation (stretch) direction (which was from left-to-right in the images), as shown for depths between 3 and $25\ \mu\text{m}$, but with decreasing amplitudes with increasing depth. However, the vectors turn orthogonal to the deformation direction at deeper locations, such as at 32 and $37\ \mu\text{m}$. Each displacement vector can be decomposed and projected on to the axes parallel and orthogonal to the deformation direction to quantify the deformation fields across the fields-of-view for these images. Their amplitudes of displacement in the parallel and orthogonal directions vs. depth are plotted in Fig. 4. Figure 4a shows the results from normal human skin, for image-pairs

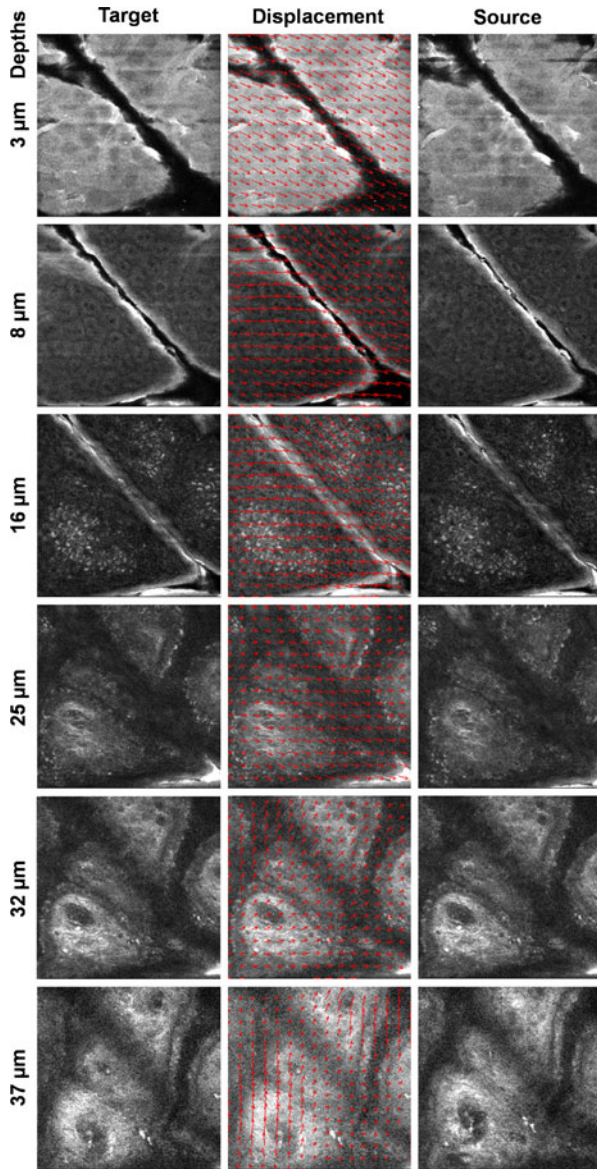


FIGURE 3. Image processing for extracting biomechanical properties. For increasing depths (3–37 μm) beneath the skin surface, target images (left column) and source images (right column) are shown before and after deformation, respectively. Target images are overlaid with displacement vectors (middle column) to show the deformation fields. The length and orientation of each arrow represents the magnitude and direction of deformation at each arrow location, and the arrow length is on the same dimensional scale as the cellular features in the images. Image size is 260 $\mu\text{m} \times 260 \mu\text{m}$ for all images.

acquired at the skin surface, and to a depth of $\sim 40 \mu\text{m}$. The amplitudes of the displacement vectors parallel to the stretch direction do not vary significantly for the first 15 μm in depth, but decrease quickly over greater depths, while the displacement amplitudes in the orthogonal direction increase at larger depths, such as at 37 μm . We applied a least-square linear fit to these

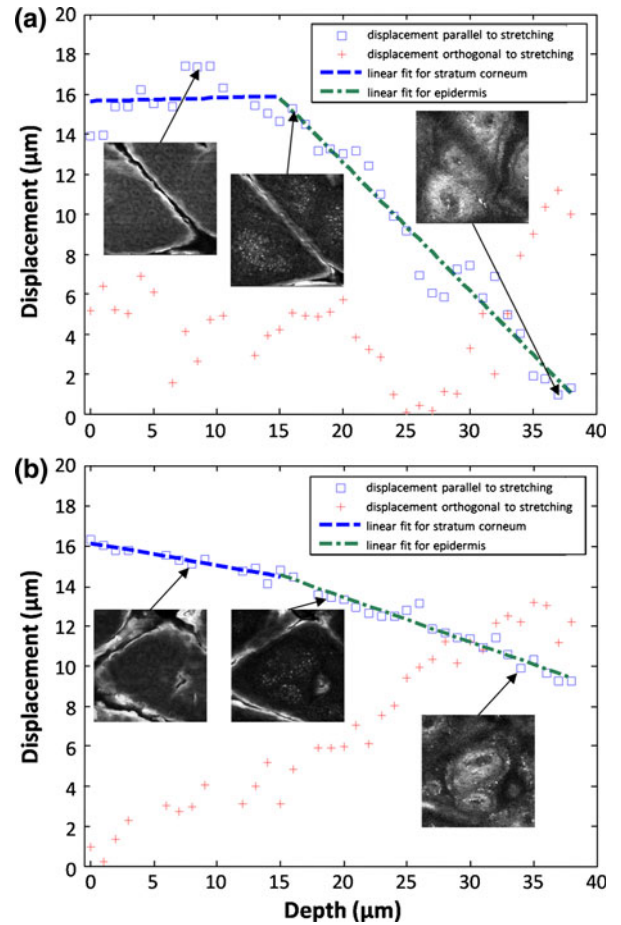


FIGURE 4. Depth-dependent biomechanical property measurements for *in vivo* human skin. (a) Results from normal baseline-state human skin. (b) Results from hydrated human skin. Square data points and cross data points represent average displacement parallel and orthogonal to the direction of stretch, respectively, at different depths. Dashed lines are linear fits to the data from different regions in depth, and MPM images are shown for selected data points at the corresponding depths.

two different regions, and the resulting slopes are clearly different. The slopes are indicative of the varying biomechanical properties between these different skin layers. The larger slopes indicate softer regions of tissue and smaller values of Young’s moduli. The results indicate that the more superficial region (0–15 μm) of human skin has a larger Young’s modulus than the deeper region (15–40 μm). From the literature, the stratum corneum layer is much stiffer in human skin, than the other parts of the epidermis,¹ which corresponds to the slope results in Fig. 4a. In our previous study using an entirely different optical diagnostic methodology, the measured Young’s modulus of normal stratum corneum was found to be 101.20 kPa, while the rest of the epidermis had a Young’s modulus of 23.01 kPa.¹⁸

To demonstrate the feasibility of our method for detecting differences in biomechanical properties *in vivo*, the same analysis was applied to hydrated skin, with results shown in Fig. 4b. It is obvious that under a hydrated condition, the slope of the fitted line representing parallel displacement amplitude vs. depth in the stratum corneum layer has a larger value than under the normal skin condition, which indicates that on the same subject and at the same skin location, this layer becomes softer as a result of the hydration process. The plot region representative of the rest of the epidermis has a smaller slope value than normal skin, which indicates that this region becomes stiffer from the hydration process. From the literature, the hydration process not only affects the superficial stratum corneum, but also affects the skin mechanical properties deeper in the epidermis, and it may increase the Young's modulus of this skin layer.^{1,18} These results suggest the feasibility of using multiphoton microscopy and this method to differentiate *in vivo* mechanical properties of tissue, using the differing mechanical properties between hydrated skin and normal skin as a representative example.

Hydration is the most important factor determining biomechanical properties in human skin layers. Keratinocytes are transported from the stratum basale outwards through the epidermis. With the same process, the keratinocytes mature, become flattened and lose water. The skin hydration decreases from ~70% at deeper epidermal regions to ~30% at the lower stratum corneum and to ~10% at the surface of the skin.³⁰ Less hydration in the stratum corneum makes this outer layer stiffer than the deeper layers. Another factor for the mechanical variation comes from intercellular material on the skin surface. In the stratum corneum, the proteins of the corneocyte cell membranes are tightly connected by a lipidic intercellular glue, which makes this skin layer more rigid.¹ However, the stratum corneum is also able to absorb an additional amount of water because of the semipermeability of the corneocyte membrane. Thus, when immersed in water, the stratum corneum will become more hydrated than normal, and subsequently become less stiff (exhibit a lower Young's modulus).

For isotropic and homogeneous samples, a uniaxial stretch applied across areas significantly larger than the image field-of-view should not create any significant deformation orthogonal to the stretch direction. However, it is not unexpected to visualize deformations in the orthogonal direction from this study on *in vivo* human skin because of the highly heterogeneous and irregular papillary layer structures present at the dermal-epidermal junction, and because of the directionality of collagen in the dermis, which defines the Langer's lines of human skin.¹⁷ Due to the complexity

of the skin structure, the orthogonal deformations also change at different sites on the skin. The complex mechanical connections and boundary conditions in human skin will affect the directionality of deformations, especially in the deeper layers and layers surrounding these dermal papillae.

In vivo human skin studies are generally affected by motion artifacts, including respiration motion, cardiac pulse motion, and other involuntary motion. In this study, however, the imaged skin regions were placed in contact with a rigidly fixed microscope sample arm, which prevented large-amplitude motion artifacts. The motion artifacts present were estimated quantitatively from experiments similar to those described above. Briefly, two 3D *in vivo* MPM stacks were acquired from the same region as above, but without mechanically stretching the skin. Then, deformation fields were taken, and displacement amplitudes from the parallel and orthogonal directions were calculated, which were 1.4 and 2.5 μm , respectively. Therefore, these motion artifacts contribute only 0.5 and 0.9%, respectively, to the results parallel to and orthogonal to the deformation directions shown in Fig. 4.

3D Image Reconstruction

The MPM image stacks were reconstructed to illustrate volumetric structures of *in vivo* human skin. One 3D reconstruction is shown in Fig. 5, where morphological features such as the microscopic skin furrows (indicated by red arrow), papilla, and cells in the stratum spinosum can be discerned. Although full 3D data sets are not compatible with the current 2D image registration algorithm, many of these morphological or cellular features may be used for 3D image registration in future studies, and thus be used to extract the 3D biomechanical properties of populations of cells in different cell layers of human skin at this microscopic scale.

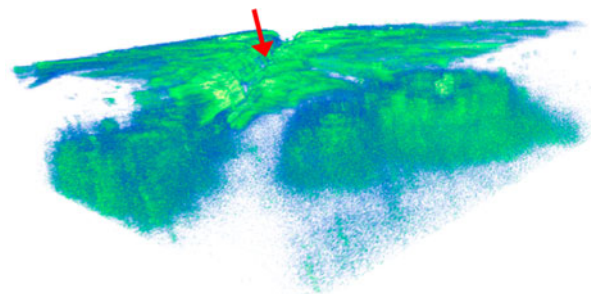


FIGURE 5. Three-dimensional reconstruction of an MPM image stack from *in vivo* human skin. A microscopic skin furrow is identified by the red arrow. Image size is $260 \mu\text{m} \times 260 \mu\text{m} \times 75 \mu\text{m}$.

CONCLUSION

Three-dimensional MPM was used to image human skin *in vivo*, and skin biomechanical properties were estimated by cell population deformations at different skin layers. Cellular features were first indentified from larger MPM mosaics, and MPM image stacks were subsequently acquired before and after stretch along the skin surface. An elastic registration algorithm was applied to the *en face* images to calculate deformation fields and displacement amplitudes both in parallel and orthogonal to the direction of stretch. Results from one human subject demonstrated that differences in *in vivo* biomechanical properties between the stratum corneum and the rest of the epidermis could be discerned in normal skin, as well as between normal and hydrated skin. These results correspond well with the literature, and reflect the physiological function of the stratum corneum. Three-dimensional MPM images were reconstructed to demonstrate volumetric features of *in vivo* human skin, and future studies will utilize the full 3D data to extract biomechanical properties between skin layers. This technique is promising for making quantitative measurements of the *in vivo* biomechanical properties of human skin, including how the barrier function of the stratum corneum may change under different conditions. This same diagnostic image-based methodology can also be used in other organs and tissues to assess the *in vivo* biomechanical properties of populations of cells under conditions of health and disease, such as in the esophagus or airway using endoscopic multiphoton microscopy techniques.

ACKNOWLEDGMENTS

We thank Dr. Haohua Tu and Eric Chaney for their laboratory assistance and thank Dr. Steven G. Adie for insightful discussions. This work was supported in part by grants from the National Institutes of Health (R01 EB005221 and RC1 CA147096) and the National Science Foundation (CBET 08-52658). Additional information can be found at <http://biophotonics.illinois.edu>.

REFERENCES

- ¹Agache, P., and P. Humbert. *Measuring the Skin*. Berlin: Springer-Verlag, pp. 96–98, 2004.
- ²Bao, G., and S. Suresh. Cell and molecular mechanics of biological materials. *Nat. Mater.* 2:715–725, 2003.
- ³Canadas, P., V. M. Laurent, C. Oddou, D. Isabey, and S. Wendling. A cellular tensegrity model to analyse the structural viscoelasticity of the cytoskeleton. *J. Theor. Biol.* 218:155–173, 2002.
- ⁴Chen, J., B. Fabry, E. L. Schiffrin, and N. Wang. Twisting integrin receptors increases endothelin-1 gene expression in endothelial cells. *Am. J. Physiol. Cell Physiol.* 280:C1475–C1484, 2001.
- ⁵Coughlin, M. F., and D. Stamenovic. A tensegrity structure with buckling compression elements: application to cell mechanics. *Trans. ASME* 64:480–486, 1997.
- ⁶Curiel-Lewandrowski, C., C. M. Williams, K. J. Swindells, S. R. Tahan, S. Astner, R. A. Frankenthaler, and S. González. Use of *in vivo* confocal microscopy in malignant melanoma: an aid in diagnosis and assessment of surgical and nonsurgical therapeutic approaches. *Arch. Dermatol.* 140:1127–1132, 2004.
- ⁷Dimitrow, E., M. Ziemer, M. J. Koehler, J. Norgauer, K. König, P. Elsner, and M. Kaatz. Sensitivity and specificity of multiphoton laser tomography for *in vivo* and *ex vivo* diagnosis of malignant melanoma. *J. Invest. Dermatol.* 129:1752–1758, 2009.
- ⁸Diridollou, S., M. Berson, V. Vabre, D. Black, B. Karlsson, F. Auriol, J. M. Gregoire, C. Yvon, L. Vaillant, Y. Gall, and F. Patat. An *in vivo* method for measuring the mechanical properties of the skin using ultrasound. *Ultrasound. Med. Biol.* 24:215–224, 1997.
- ⁹Ericson, M. B., C. Simonsson, S. Guldbrand, C. Ljungblad, J. Paoli, and M. Smedh. Two-photon laser-scanning fluorescence microscopy applied for studies of human skin. *J. Biophoton.* 1:320–330, 2008.
- ¹⁰Evans, E., and A. Yeung. Apparent viscosity and cortical tension of blood granulocytes determined by micropipet aspiration. *Biophys. J.* 56:151–160, 1989.
- ¹¹Graf, B. W., Z. Jiang, H. Tu, and S. A. Boppart. Dual-spectrum laser source based on fiber continuum generation for integrated optical coherence and multiphoton microscopy. *J. Biomed. Opt.* 14:034019, 2009.
- ¹²Ingber, D. E. Mechanical signaling and the cellular response to extracellular matrix in angiogenesis and cardiovascular physiology. *Circ. Res.* 91:877–887, 2002.
- ¹³Koehler, M. J., K. König, P. Elsner, R. Bückle, and M. Kaatz. *In vivo* assessment of human skin aging by multiphoton laser scanning tomography. *Opt. Lett.* 31: 2879–2881, 2006.
- ¹⁴König, K., A. Ehlers, F. Stracke, and I. Riemann. *In vivo* drug screening in human skin using femtosecond laser multiphoton tomography. *Skin Pharmacol. Physiol.* 19: 78–88, 2006.
- ¹⁵König, K., and I. Riemann. High-resolution multiphoton tomography of human skin with subcellular spatial resolution and picosecond time resolution. *J. Biomed. Opt.* 8:432–439, 2003.
- ¹⁶Krehbiel, J., J. Lambros, J. Viator, and N. R. Sottos. Digital image correlation for improved detection of basal cell carcinoma. *Exp. Mech.* 2009. doi:10.1004/s11340-009-9324-8.
- ¹⁷Langer, K. On the anatomy and physiology of the skin I. The cleavability of the cutis. *Br. J. Plast. Surg.* 31:3–8, 1978.
- ¹⁸Liang, X., and S. A. Boppart. Biomechanical properties of *in vivo* human skin from dynamic optical coherence elastography. *IEEE Trans. Biomed. Eng.* 57:953–959, 2010.
- ¹⁹Liang, X., B. W. Graf, and S. A. Boppart. Multimodality microscopy for imaging three-dimensional engineered and natural tissues. *J. Biophoton.* 2:643–655, 2009.
- ²⁰Liu, Z., N. J. Sniadecki, and C. S. Chen. Mechanical forces in endothelial cells during firm adhesion and early

- transmigration of human monocytes. *Cell. Mol. Bioeng.* 3:50–59, 2010.
- ²¹Mann, C., and D. Leckband. Measuring traction forces in long-term cell cultures. *Cell. Mol. Bioeng.* 3:40–49, 2010.
- ²²Marcellier, H., P. Vescovo, D. Varchon, P. Vacher, and P. Humbert. Optical analysis of displacement and strain fields on human skin. *Skin Res. Technol.* 7:246–253, 2001.
- ²³Mathur, A. B., A. M. Collinsworth, W. M. Reichert, W. E. Kraus, and G. A. Truskey. Endothelial, cardiac muscle and skeletal muscle exhibit different viscous and elastic properties as determined by atomic force microscopy. *J. Biomech.* 34:1545–1553, 2001.
- ²⁴Pena, A., M. Strupler, T. Boulesteix, and M. Schanne-Klein. Spectroscopic analysis of keratin endogenous signal for skin multiphoton microscopy. *Opt. Express* 13:6268–6274, 2005.
- ²⁵Rajadhyaksha, M., S. González, J. M. Zavislan, R. R. Anderson, and R. H. Webb. *In vivo* confocal scanning laser microscopy of human skin II: advances in instrumentation and comparison with histology. *J. Invest. Dermatol.* 113: 293–303, 1999.
- ²⁶Sánchez Sorzano, C. Ó., P. Thévenaz, and M. Unser. Elastic registration of biological images using vector-Spline regularization. *IEEE Trans. Biomed. Eng.* 52:652–663, 2005.
- ²⁷Satcher, R. L., and C. F. Dewey, Jr. Theoretical estimates of mechanical properties of the endothelial cell cytoskeleton. *Biophys. J.* 71:109–118, 1996.
- ²⁸Staloff, I. A., E. Guan, S. Katz, M. Rafailovitch, A. Sokolov, and S. Sokolov. An *in vivo* study of the mechanical properties of facial skin and influence of aging using digital image speckle correlation. *Skin Res. Technol.* 14:127–134, 2008.
- ²⁹Svoboda, K., and S. M. Block. Biological applications of optical forces. *Annu. Rev. Biophys. Biomol. Struct.* 23:247–285, 1994.
- ³⁰Verdier-Sevrain, S., and B. Frederic. Skin hydration: a review on its molecular mechanisms. *J. Cosmet. Dermatol.* 6:75–82, 2007.
- ³¹Vinegoni, C., T. S. Ralston, W. Tan, W. Luo, D. L. Marks, and S. A. Boppart. Integrated structural and functional optical imaging combining spectral-domain optical coherence and multiphoton microscopy. *Appl. Phys. Lett.* 88: 053901, 2006.